crystals

MDPI

Article

The Crystal Structure of Manganotychite, $Na_6Mn_2(CO_3)_4(SO_4)$, and Structural Relations in the Northupite Group

Sergey V. Krivovichev [1,2,*], Taras L. Panikorovskii [1,2], Ayya V. Bazai [1] and Mikhail Yu. Sidorov [3]

[1] Nanomaterials Research Centre, Kola Science Centre, Russian Academy of Sciences, Fersmana 14, 184209 Apatity, Russia
[2] Department of Crystallography, Institute of Earth Sciences, St. Petersburg State University, University Emb. 7/9, 199034 St. Petersburg, Russia
[3] Geological Institute, Kola Science Centre, Russian Academy of Sciences, Fersmana 14, 184209 Apatity, Russia
* Correspondence: s.krivovichev@ksc.ru

Abstract: The crystal structure of manganotychite has been refined using the holotype specimen from the Alluaiv Mountain, Lovozero massif, Kola peninsula, Russia. The mineral is cubic, $Fd\bar{3}$, a = 14.0015(3) Å, V = 2744.88(18) Å^3, Z = 8, R_1 = 0.020 for 388 independently observed reflections. Manganotychite is isotypic to tychite and ferrotychite. Its crystal structure is based upon a three-dimensional infinite framework formed by condensation of MnO_6 octahedra and CO_3 groups by sharing common O atoms. The sulfate groups and Na^+ cations reside in the cavities of the octahedral-triangular metal-carbonate framework. In terms of symmetry and basic construction of the octahedral-triangular framework, the crystal structure of manganotychite is identical to that of northupite, $Na_3Mg(CO_3)_2Cl$. The transition northupite → tychite can be described as a result of the multiatomic $2Cl^- \rightarrow (SO_4)^{2-}$ substitution, where both chlorine and sulfate ions are the extra-framework constituents. However, the positions occupied by sulfate groups and chlorine ions correspond to different octahedral cavities within the skeletons of Na atoms. The crystal structure of northupite can be considered as an interpenetration of two frameworks: anionic $[Mg(CO_3)_2]^{2-}$ octahedral-triangular framework and cationic $[ClNa_3]^{2-}$ framework with the antipyrochlore topology. Both manganotychite and northupite structure types can be described as a modification of the crystal structure of diamond (or the **dia** net) via the following steps: (i) replacement of a vertex of the **dia** net by an M_4 tetrahedron (no symmetry reduction); (ii) attachment of (CO_3) triangles to the triangular faces of the M_4 tetrahedra (accompanied by the $Fd\bar{3}m \rightarrow Fd\bar{3}$ symmetry reduction); (iii) filling voids of the resulting framework by Na^+ cations (no symmetry reduction); and (iv) filling voids of the Na skeleton by either sulfate groups (in tychite-type structures) or chlorine atoms (in northupite). As a result, the information-based structural complexity of manganotychite and northupite exceeds that of the **dia** net.

Keywords: manganotychite; northupite group; crystal structure; tychite; ferrotychite; antiperovskite; antipyrochlore; diamond net; structural complexity

Citation: Krivovichev, S.V.; Panikorovskii, T.L.; Bazai, A.V.; Sidorov, M.Y. The Crystal Structure of Manganotychite, $Na_6Mn_2(CO_3)_4(SO_4)$, and Structural Relations in the Northupite Group. *Crystals* **2023**, *13*, 800. https://doi.org/10.3390/cryst13050800

Academic Editor: Zhaohui Li

Received: 5 April 2023
Revised: 5 May 2023
Accepted: 7 May 2023
Published: 10 May 2023

1. Introduction

The northupite group of minerals contains four mineral species: northupite, tychite, ferrotychite, and manganotychite. Historically, the first mineral of the group was northupite, $Na_3Mg(CO_3)_2Cl$, discovered in Borax Lake, California, by C.H. Northup and described by Foote in 1895 [1] and Pratt in 1896 [2]. Its sulfate analogue, tychite, $Na_6Mg_2(CO_3)_4(SO_4)$, was described several years later from the same locality and the same sample [3,4]. Later, both minerals have been found in other saline lakes [5–7], e.g., Lake Katwe, Uganda [8]. A.P. Khomyakov and coauthors described Fe and Mn analogues of tychite, which were named ferrotychite, $Na_6Fe_2(CO_3)_4(SO_4)$ [9], and manganotychite, $Na_6Mn_2(CO_3)_4(SO_4)$ [10], respectively. Ferrotychite was found in the Oleniy Ruchey mineral deposit in the Eastern

part of the Khibiny alkaline massif, Kola peninsula, Russia, whereas manganotychite was described from the underground workings of the Alluaiv mountain, North-Western part of the Lovozero alkaline massif, Kola peninsula, Russia. In both cases, the formation of minerals was associated with the late stages of hydrothermal crystallization from solutions enriched by alkali and fugitive components of the alkali silicate liquids [9,10]. Recently tychite [11] and northupite [12] were described from melt inclusions in olivine from mantle xenoliths of kimberlite pipes from Siberia, Russia.

The investigations of the crystal chemical and spectroscopic properties of the northupite-group minerals started in 1931 when Gossner and Koch [13] and Shiba and Watanabé [14] provided preliminary structural models for northupite. In particular, Shiba and Watanabé [14] attempted to solve the structure of tychite in the space group $Fd\bar{3}m$. The correct space group, $Fd\bar{3}$, was determined by Gossner and Koch [13]. Watanabé [15] solved the crystal structures of both tychite and northupite in the $Fd\bar{3}$ space group with the subsequent refinements for northupite and tychite provided by Dal Negro et al. [16] and Schmidt et al. [17]. The crystal structure of ferrotychite was refined by Malinovskii et al. [18]. Spectroscopic properties of the northupite-group minerals have been studied in a number of works [17,19]. In the most recent work, Sidorov et al. [20] reported Raman spectra for tychite, manganotychite, and ferrotychite.

It is worthy of note that synthetic compounds with the northupite-type structure have been actively investigated recently due to their remarkable magnetic properties [21–23]. When the divalent metal sites are occupied by magnetic ions (Co^{2+} or Mn^{2+}), these ions form a so-called pyrochlore lattice consisting of the framework of corner-sharing M_4 tetrahedra (M = Co^{2+} or Mn^{2+}) that form a cristobalite-type arrangement with the diamond topology. For the cobalt analogue of northupite, $Na_3Co(CO_3)_2Cl$, the coexistence of magnetic order and spin-glass state have been reported by Fu et al. [22]; whereas for $Na_3Mn(CO_3)_2Cl$, no signature of a spin-glass transition or magnetic order had been detected [23].

In this paper, we provide the results of a single-crystal diffraction study of manganotychite, the only natural member of the northupite group that had not been characterized structurally. In addition, we discuss structural relations in the northupite group, in particular, the structural aspects of the chlorine-for-sulfate substitution and antiperovskite (antipyrochlore) features of the northupite structure type.

2. Materials and Methods

2.1. Sample Description and Composition

The sample of manganotychite used in this study is the holotype specimen deposited by A.P. Khomyakov at the Geological and Mineralogical Museum of the Geological Institute, Kola Science Centre of the Russian Academy of Sciences, Apatity, Russia (catalogue no. GIM 6379). The sample originated from the Alluaiv Mountain, Lovozero massif, Kola peninsula, Russia (Figure 1a,b) and was found in intensely mineralized pegmatitic formations close to pegmatites [24]. They are represented by well-shaped veins up to 0.3 m thick in poikilitic nepheline-sodalite syenites. The veins are composed of coarse-grained (1–5 cm) aggregates of microcline, cancrinite, aegirine, and a wide range of salt minerals: villiaumite, cryolite, kogarkoite, trona, shortite, sidorenkite, and manganotychite. Less widespread minerals of this group are nahcolite, wegscheiderite, thermonatrite, pirssonite, burbankite, rhodochrosite, and neighborite. Other minerals in the veins are nepheline, sodalite, analcime, albite, natrolite, lorenzenite, lamprophyllite, eudialyte, catapleite, zircon, neptunite, serandite, leucosphenite, leifite, apatite, fluorite, cleiophane, galena, pyrite, and ilmenite. Manganotychite aggregates are mainly confined to the axial zones of veins, where they form nests of blows, up to 10–15 cm with glassy lustre (Figure 1c).

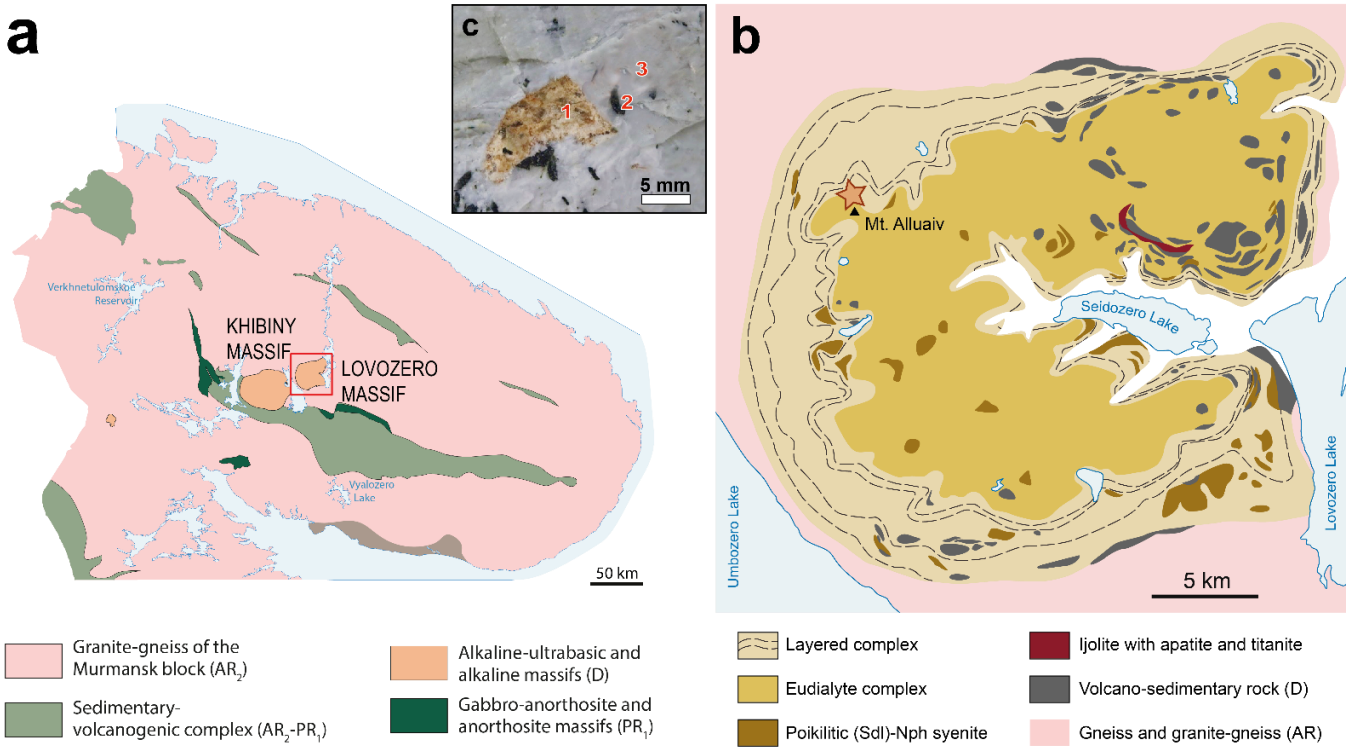

Figure 1. Geology of the Lovozero massif after with modification (**a**) and type locality of manganotychite marked by an orange star (**b**), photo of the greyish irregular grains of manganotychite (1) with arfvedsonite (2) in albite (3) matrix (**c**). Reprinted from [25] under the Creative Commons Attribution (CC BY) license 4.0.

The composition of manganotychite was studied by Cameca MS-46 microprobe (Cameca, Gennevilliers, France) operated in a WDS mode at 22 kV and 20–40 nA and a beam diameter of 10 μm with counting times of 20 s (for a peak) and 2 × 10 s (for background before and after the peak), with 5–10 counts for every element in each point. The following standards were used: lorenzenite (Na), pyrope (Mg), barite (S), $MnCO_3$ (Mn), and hematite (Fe). The CO_3 content was calculated based on the crystal structure refinement.

The mean chemical composition (FeO 4.25, MnO 16.67, MgO 2.04, Na_2O 31.94, SO_3 14.22, and CO_2 30.65, sum 99.77 wt. %) measured from 5 spots and normalized on 16 O atoms is $Na_{5.92}(Mn_{1.35}Fe_{0.34}Mg_{0.29})_{\Sigma 1.98}S_{1.02}C_{4.00}O_{16.00}$, which is in agreement with the results of the single-crystal diffraction study (see below). The Raman spectra for the sample were reported by Sidorov et al. [20].

2.2. Single-Crystal X-ray Diffraction

A single-crystal X-ray diffraction study was done on the same sample of manganotychite that was used for the Raman spectroscopic study as reported by Sidorov et al. [20]. The X-ray diffraction data were collected by means of an XtaLAB Synergy-S diffractometer (Rigaku corp., Tokyo, Japan) equipped with a hybrid photon counting detector HyPix-6000HE at the Centre of the Collective Use of Equipment, Kola Science Centre. The data were integrated and corrected by means of the CrysAlisPro [26] program package, which was also used to apply an empirical absorption correction using spherical harmonics, as implemented in the SCALE3 ABSPACK scaling algorithm. The SHELXL program [27] was used for the crystal structure refinement. The structure of manganotychite was refined to R_1 = 0.021 for 388 independent reflections with $F_{obs} > 4\sigma(F_{obs})$. The refined occupancy of the divalent metal M site is $Mn_{0.87}Mg_{0.13}$, which agrees well with the occupancy of $Mn_{0.60}Fe_{0.25}Mg_{0.15}$ derived from the empirical chemical data, taking into account close proximity between the site-scattering powers of Mn and Fe. Crystal data, data collection

information, and structure refinement details are given in Table 1, and atom coordinates and selected interatomic distances are in Tables 2 and 3, respectively.

Table 1. Crystal data and structure refinement for manganotychite.

Temperature/K	293(2)
Crystal system	cubic
Space group	$Fd\bar{3}$
a/Å	14.0015(3)
Volume/Å^3	2744.88(18)
Z	8
D_{calc}, g/cm^3	2.788
μ/mm^{-1}	2.071
F(000)	2245.0
Crystal size/mm^3	0.18 × 0.14 × 0.14
Radiation	Mo$K\alpha$ (λ = 0.71073)
2Θ range for data collection/°	8.234 to 65.960
Index ranges	$-15 \leq h \leq 21$, $-16 \leq k \leq 12$, $-20 \leq l \leq 8$
Reflections collected	1340
Independent reflections	388 [R_{int} = 0.0182, R_{sigma} = 0.0166]
Data/restraints/parameters	388/0/26
Goodness-of-fit on F^2	1.129
Final R indices [I ≥ 2σ (I)]	R_1 = 0.0201, wR_2 = 0.0532
Final R indices [all data]	R_1 = 0.0214, wR_2 = 0.0536
Largest diff. peak/hole/e Å^{-3}	0.24/−0.51

Table 2. Atomic coordinates, site-occupancy factors (s.o.f.s), and equivalent isotropic displacement parameters (10^{-4} Å^2) for manganotychite.

Site	s.o.f.	*x*/*a*	*y*/*b*	*z*/*c*	U_{iso}
M	$Mn_{0.87}Mg_{0.13}$	$\frac{1}{2}$	$\frac{1}{2}$	$\frac{1}{2}$	0.0092(2)
S	S	3/8	1/8	3/8	0.0121(2)
Na	Na	3/8	0.65892(5)	3/8	0.0193(2)
O1	O	0.31404(6)	0.81404(6)	0.43596(6)	0.0194(3)
O2	O	0.48237(6)	0.52891(5)	0.34933(5)	0.0137(2)
C	C	0.47028(7)	0.47028(7)	0.27972(7)	0.0098(3)

Table 3. Selected interatomic distances (Å) for the crystal structure of manganotychite.

M–O	2.1622(8) 6×	Na–O1	2.4108(8) 2×
S–O	1.4784(14) 4×	Na–O2	2.3880(10) 2×
C–O	1.2855(7) 3×	Na–O1	2.4848(7) 2×
		<Na–O>	2.4279

3. Results

3.1. Structure Description

The crystal structure of manganotychite is isotypic to those of tychite [17] and ferrotychite [18]. In their review on the crystal chemistry of sulfates, Hawthorne et al. [28] classified the structure of ferrotychite as based upon infinite heteropolyhedral framework, though, technically speaking, sulfate groups do not participate in the framework construction, but reside within the cavities of the framework formed by MO_6 octahedra and CO_3 triangular groups.

The crystal structure of manganotychite is shown in Figure 2a. It is based upon a three-dimensional infinite framework formed by the condensation of MnO_6 octahedra and CO_3 groups by sharing common O atoms. The fundamental building block (FBB) of the framework has a tetrahedral shape and is formed by four MnO_6 octahedra and four CO_3 triangles that are linked by common O atoms (Figure 2b,c) so that the four Mn atoms and four C atoms are arranged at the vertices of a distorted cube (a cubane arrangement).

The adjacent FBBs are linked through common MnO_6 octahedra so that each octahedron belongs to two FBBs. The core of each FBB is an 'empty' Mn_4 tetrahedron (Figure 2d). The Mn_4 tetrahedra share corners to produce a highly symmetrical pyrochlore-type network (Figure 2e), which is a maximum-symmetry version of cristobalite topology, which, in turn, is a derivative of diamond topology. The diamond net (**dia**) is one of the simplest and most common topologies in inorganic and metal-organic framework materials [29].

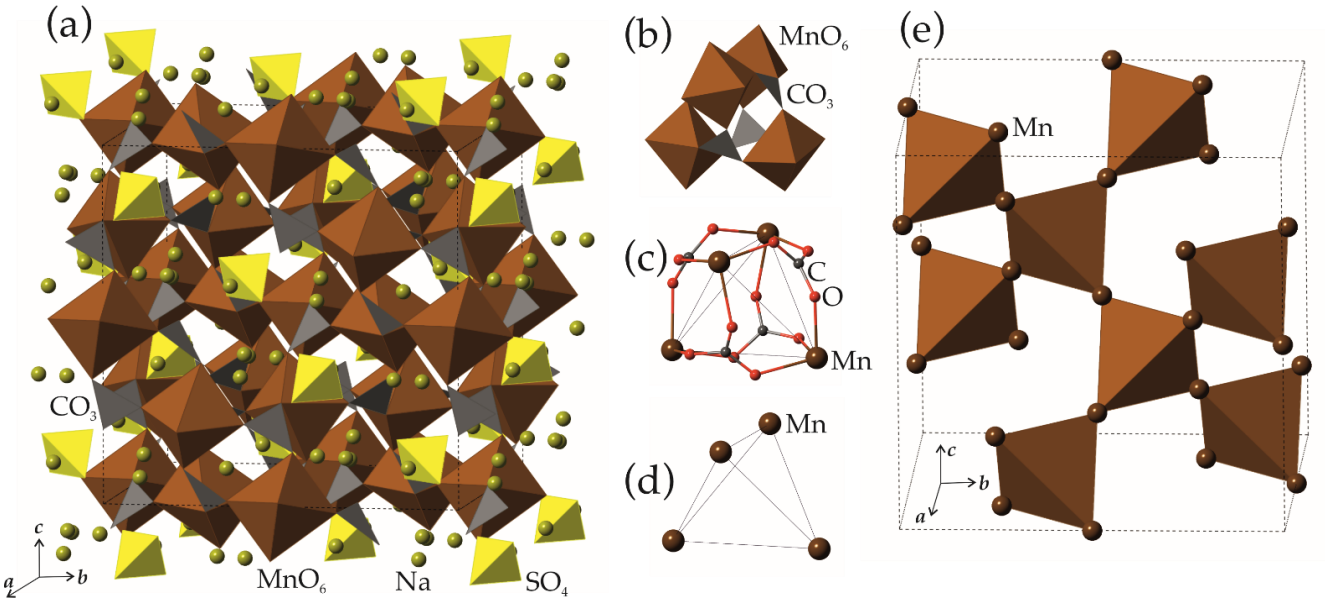

Figure 2. The crystal structure of manganotychite (**a**), the tetrahedral FBB formed by MnO_6 octahedra and CO_3 groups shown in polyhedral (**b**) and ball-and-stick modes (**c**), the Mn_4 tetrahedron (**d**) at the core of the FBBs shown in (**b**,**c**), and the pyrochlore framework (**e**) formed by corner-sharing Mn_4 tetrahedra. Legend: MnO_6 octahedra = brown, SO_4 tetrahedra = yellow, CO_3 triangles = grey; Mn, Na, O, and C atoms are shown as brown, greenish-yellow, red and grey spheres, respectively.

The sulfate groups and Na^+ cations reside in the cavities of the octahedral-triangular metal carbonate framework.

3.2. X-ray Diffraction versus Raman Spectroscopic Study

The Raman spectrum of manganotychite studied in this work was reported and characterized in detail by Sidorov et al. [20]. The Raman bands observed for the mineral are in good agreement with the results of the single crystal X-ray diffraction study. The spectrum is dominated by the bands typical for the internal vibrations of the carbonate and sulfate groups. The bands at 209 and 233 cm^{-1} belong to lattice vibrations. The internal vibrations of sulfate groups are responsible for the appearance of bands at 967 cm^{-1} (symmetrical v_1 vibrations), 1136 cm^{-1} (asymmetrical v_3 vibrations), and 464, 614, 630 cm^{-1} (deformation v_2 and v_4 vibrations). The bands at 711, 1095, and 1419 cm^{-1} correspond to the v_4, v_1, and v_3 vibrations of carbonate groups, respectively.

3.3. Structural Relations

In terms of symmetry and basic construction of the octahedral-triangular framework, the crystal structure of manganotychite (as well as those of tychite and ferrotychite) is identical to those of northupite, $Na_3Mg(CO_3)_2Cl$ and related inorganic compounds (see above). The transition northupite → tychite can be described as a result of the multiatomic $2Cl^- \rightarrow (SO_4)^{2-}$ substitution, where both chlorine and sulfate ions are the extra-framework constituents. However, the positions occupied by sulfate groups and chlorine ions within the framework are different, which is depicted in Figure 2 in terms of the arrangement of Na atoms. In both tychite and northupite structure types, Na atoms form identical

arrangements corresponding to the arrangement of O atoms of an octahedral framework in a classical cubic pyrochlore $A_2B_2O_7 = [A_2O'][B_2O_6]$, where $[A_2O']$ is a pyrochlore network of oxocentered ($O'A_4$) tetrahedra [30] and $[B_2O_6]$ is a framework of corner-sharing (BO_6) octahedra. In both northupite and tychite, Na atoms form a skeleton with Na_6 octahedral cavities of two types. In the cluster shown in Figure 3, the octahedral cavity of the first type is a Na_6 octahedron flattened parallel to one of its threefold axes. This octahedron is empty in manganotychite (Figure 3a) and occupied by Cl atoms in northupite (Figure 3b). The flattening character of this octahedral cavity is manifested in the difference between Na–Na distances, as it has six Na–Na edges of 3.564 Å (in both structures), and six Na-Na edges of 4.279 Å (in manganotychite) and 4.522 Å (in northupite). The second octahedral cavity is a regular Na_6 octahedron with equal twelve Na–Na edges of 4.279 Å (in manganotychite) and 4.522 Å (in northupite). The smaller size of this cavity in northupite is explained by its occupancy by a sulfate group (Figure 3a). The same cavity in northupite is empty.

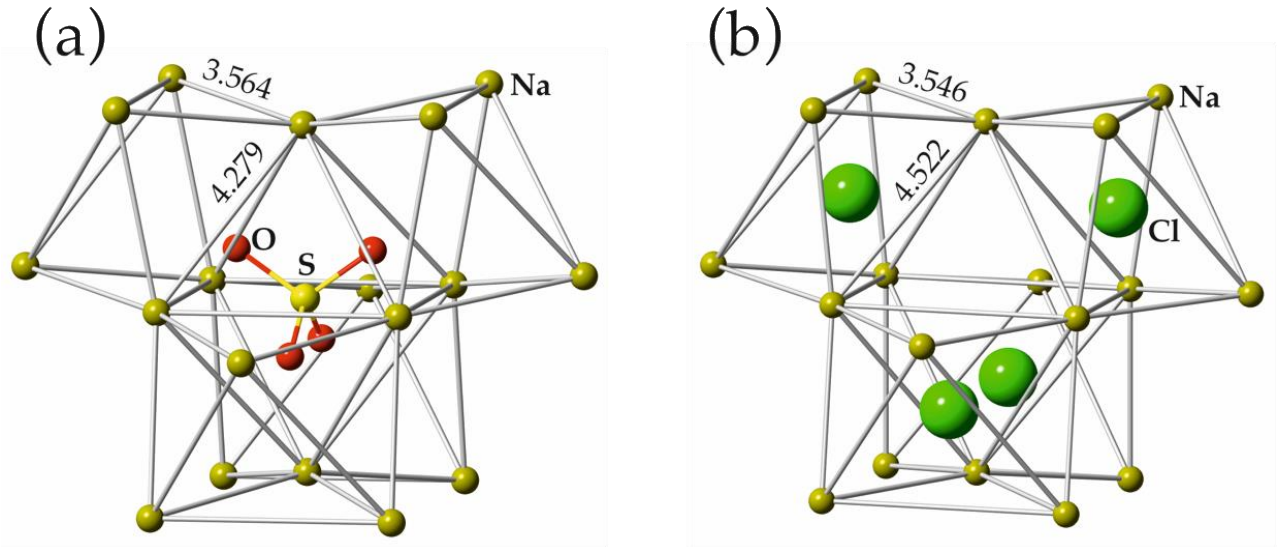

Figure 3. The positions of the sulfate group in the crystal structure of manganotychite (**a**) and of chlorine ions in northupite (**b**) relative to the skeleton of Na atoms (shown in dark yellow). Legend: S = light-yellow; O = red; Cl = green. The Na-Na distances (in Å) are given near the respective Na–Na contacts.

The occupancy of the flattened Na_6 octahedra by Cl anions in northupite (Figure 3b) allows for the consideration of ($ClNa_6$) octahedra as separate coordination polyhedra and to analyse their connectivity. It is of interest that the ($ClNa_6$) octahedra share corners to form in northupite and its synthetic analogues an octahedral framework similar to the $[B_2O_6]$ framework observed in cubic pyrochlores $A_2B_2O_7 = [A_2O'][B_2O_6]$. However, in contrast to the latter, where the framework is formed by cation-centred (BO_6) octahedra, the framework in northupite is formed by anion-centred ($ClNa_6$) octahedra. This allows for the consideration of the respective $[Cl_2Na_6]$ framework in northupite as an antipyrochlore or an inverse pyrochlore, by analogy with antiperovskites or inverse perovskites [31]. Similar antipyrochlore frameworks formed by N-centered metal octahedra are known in alkaline earth metal nitrides [32,33] and by O-centered (OTi_6) octahedra in $Ti_2[Ti_3O]_2(Pd)_4$ [34].

Thus, the crystal structure of northupite and its synthetic analogues can be described as consisting of the antipyrochlore-type octahedral framework $[Cl_2Na_6]^{4+}$ formed by ($ClNa_6$) octahedra (Figure 4a) and the $[M_2(CO_3)_4]^{4-}$ octahedral-triangular framework (Figure 4b; M = Mg, Co, Mn). In the whole crystal structure, the anionic and cationic frameworks of the two types interpenetrate (Figure 4c).

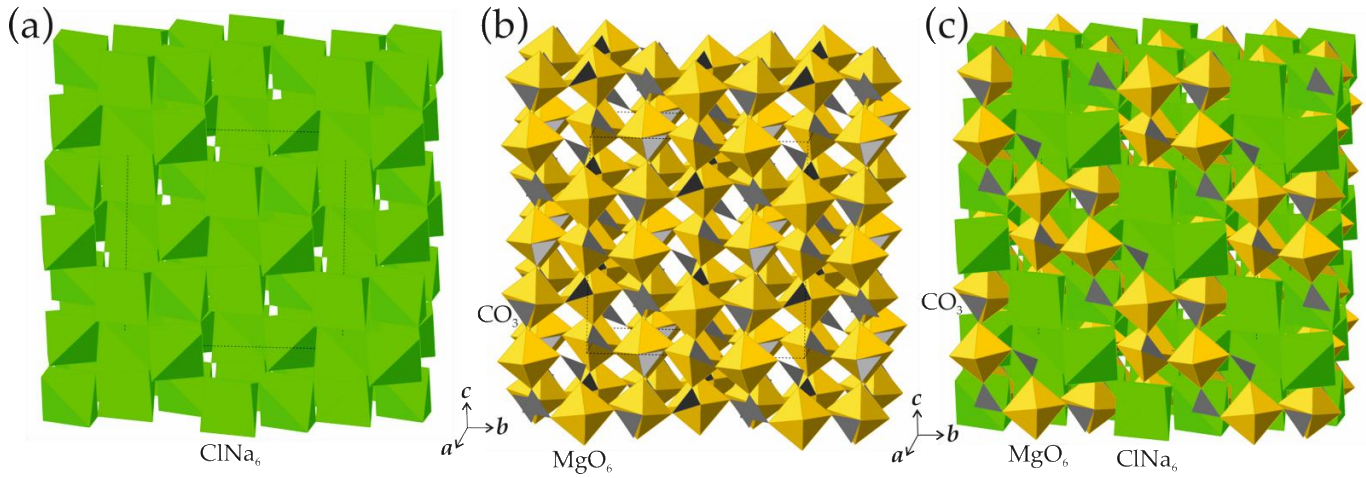

Figure 4. The crystal structure of northupite: the antipyrochlore-type octahedral framework formed by ($ClNa_6$) octahedra (**a**), the [$Mg(CO_3)_2$] octahedral-triangular framework (**b**), and their interpenetration in the whole structure (**c**). Legend: ($ClNa_6$) octahedra, (MgO_6) octahedra, and (CO_3) groups are shown as green, yellow, and gray, respectively.

4. Discussion

The northupite-group minerals and related synthetic northupite-type compounds belong to two structure types that correspond to the chemical formulas, $Na_3M(CO_3)_2Cl$ or $Na_6M_2(CO_3)_4Cl_2$ (M = Mg, Fe, Mn) and $Na_6M_2(CO_3)_4(SO_4)$ (M = Mg, Mn, Co). The transition between the two structure types can be described by the $2Cl^- \rightarrow (SO_4)^{2-}$ substitution, which, as to our knowledge, has not been observed so far either in nature or under laboratory conditions. Among mineral species, the only mineral of the second structure type is northupite (M = Mg), and other members of the group (M = Mn, Fe) can be expected to exist in nature, by analogy with tychite, ferrotychite, and manganotychite.

The genealogy of both structure types originates from the diamond-like **dia** net, which is one of the five simplest nets observed in inorganic and metal–organic compounds. The complexity of the **dia** net considered as the Shannon information amount that takes into account vertices and edges [35–37] is equal to 0.918 bits per element (vertex or edge) and 5.510 bits per unit cell. The atomic structural complexities of the $Na_3M(CO_3)_2Cl$ and $Na_6M_2(CO_3)_4(SO_4)$ structure types are equal to 1.988 and 2.219 bits per atom, respectively, whereas their total structural complexities are 103.364 and 128.704 bits per unit cell, respectively. Taking into account that both structure types contain the same $[M_2(CO_3)_4]^{4-}$ octahedral-triangular anionic framework and the same amount of Na^+ cations, the difference is due to the $2Cl^- \rightarrow (SO_4)^{2-}$ substitution, which corresponds to the larger number of atoms for tychite-type structures and the lower number of atoms for northupite-type structures. The rise of complexity from the **dia** net to the $Na_3M(CO_3)_2Cl$ and $Na_6M_2(CO_3)_4(SO_4)$ structure types is due to the various modifications of the net through the introduction of different atomic groups. The latter is accompanied by the decrease of the symmetry from the $Fd\bar{3}m$ space group for the **dia** net to the $Fd\bar{3}$ space group.

The set of modifications corresponding to the transition from the **dia** net to the $Na_3M(CO_3)_2Cl$ and $Na_6M_2(CO_3)_4(SO_4)$ structure types can be described as follows: (i) replacement of a vertex of the **dia** net by an M_4 tetrahedron (no symmetry reduction); (ii) attachment of (CO_3) triangles to the triangular faces of M_4 tetrahedra (Figure 2c) (accompanied by the $Fd\bar{3}m \rightarrow Fd\bar{3}$ symmetry reduction); (iii) filling voids of the resulting framework by Na^+ cations (no symmetry reduction); and (iv) filling voids of the Na skeleton by either sulfate groups (in tychite-type structures) or chlorine atoms (in northupite).

It is remarkable that, at the bottom, the structural topologies of the northupite-group minerals relate to such a simple and highly symmetric structure as that of a diamond.

It is of interest to investigate the position of manganotychite, tychite, and ferrotychite among the known sulfate carbonates. There are, in total, 26 known mineral species that have crystallographically well-defined carbonate and sulfate groups. Among them, only five do not contain hydrogen in any form (manganotychite, tychite, ferrotychite, burkeite, and hanksite), whereas 13 are hydrates, i.e., contain symmetrically independent H_2O molecules in their crystal structures. The latter minerals include such remarkable rarities as ramazzoite, $[Mg_8Cu^{2+}{}_{12}(PO_4)(CO_3)_4(OH)_{24}(H_2O)_{20}][(H_{0.33}S^{6+}O_4)_3(H_2O)_{36}]$ [38], and putnisite, $SrCa_4Cr^{3+}{}_8(CO_3)_8(SO_4)(OH)_{16}\cdot 25H_2O$ [39], both containing polyoxometalate units in their crystal structures [40]. It is worthy of note that, in ramazzoite, the polyoxometalate clusters contain phosphate and carbonate groups, whereas sulfate groups provide the linkage between polycationic units. The same situation is observed in putnisite as well, where the polyoxometalate cluster has the composition $[Cr^{3+}{}_8(OH)_{16}(CO_3)_8]^{8-}$. In this cluster, eight Cr^{3+}-centered octahedra share edges to form a ring, which is decorated by eight (CO_3) triangles. This wheel-shaped cluster has no analogues among minerals and synthetic compounds. Putnisite is a secondary mineral formed during the oxidation of the primary sulfide-bearing rocks, whereas ramazzoite crystallized from low-temperature (<50 °C) aqueous solutions at pH from 6 to 12 and low fugacity of CO_2 [38]. Both ramazzoite and putnisite possess a high structural complexity with 1848.162 and 2932.730 bits of information per reduced unit cell, respectively.

According to their paragenetic modes [41], most of the known sulfate carbonate minerals are secondary in origin and formed as a result of low-temperature subaerial oxidative hydration and weathering. Only five minerals (tychite, ferrotychite, manganotychite, burkeite, and hanksite) are considered as primary, occurring either in evaporites and saline lakes (tychite, burkeite, $Na_4(SO_4)(CO_3)$, and hanksite, $KNa_{22}(SO_4)_9(CO_3)_2Cl$) or as late-stage minerals in the ultra-alkali and agpaitic igneous rocks (ferrotychite and manganotychite). All five primary sulfate carbonate minerals contain Na as an essential mineral-forming component that indicates the importance of high Na potential for their formation.

Author Contributions: Conceptualization, S.V.K.; methodology, T.L.P. and M.Y.S.; formal analysis, S.V.K., A.V.B. and T.L.P.; investigation, T.L.P., A.V.B. and M.Y.S.; writing—original draft preparation, S.V.K.; writing—review and editing, S.V.K., T.L.P. and M.Y.S.; funding acquisition, S.V.K. All authors have read and agreed to the published version of the manuscript.

Funding: This research was funded by the Russian Science Foundation, grant 19-17-00038.

Data Availability Statement: The raw data on chemical composition and crystal structure are available from the authors upon request.

Acknowledgments: The X-ray diffraction measurements were performed in the Centre for the Collective Use of Equipment of Kola Science Centre, Russian Academy of Sciences.

Conflicts of Interest: The authors declare no conflict of interest.

References

1. Foote, W.M. Preliminary note on a new alkali mineral. *Am. J. Sci.* **1895**, *150*, 480–481. [CrossRef]
2. Pratt, J.H. On northupite; pirssonite, a new mineral; Gaylussite and hanksite from Borax Lake, San Bernardino County, California. *Am. J. Sci.* **1896**, *152*, 123–135. [CrossRef]
3. Penfield, S.L.; Jamieson, G.S. On tychite, a new mineral from Borax Lake, California, and on its artificial production and its relations to northupite. *Am. J. Sci.* **1905**, *20*, 217–224. [CrossRef]
4. Penfield, S.L.; Jamieson, G.S. Über Tychit, ein neues Mineral vom Boraxsee in Californien, seine künstliche Darstellung und seine Beziehungen zum Northupit. *Z. Krystallogr. Miner.* **1906**, *41*, 235–242. [CrossRef]
5. Fahey, J.J.; Mrose, M.E. Saline minerals of the Green River formation, with a section on X-ray powder data for saline materials of the Green River formation. *USGS Prof. Paper* **1962**, *405*, 50.
6. Marchesini, M.; Barresi, A. The Wadi Natrun evaporite deposits, Western Desert, Buhayra Governate, Egypt. *Mineral. Rec.* **2019**, *50*, 723–748.

7. Yu, K.-H.; Cao, Y.-C.; Qiu, L.-W.; Sun, P.-P.; Yang, Y.-Q.; Qu, C.-S.; Li, Y.-W.; Wan, M.; Su, Y.-G. Brine Evolution of Ancient Lake and Mechanism of Carbonate Minerals during the Sedimentation of Early Permian Fengcheng Formation in Mahu Depression, Junggar Basin, China. *Nat. Gas Geosci.* **2016**, *27*, 1248–1263.
8. Kasedde, H.; Kirabira, J.B.; Bäbler, M.U.; Tilliander, A.; Jonsson, S. Characterization of brines and evaporites of Lake Katwe, Uganda. *J. Afr. Earth Sci.* **2014**, *91*, 55–65. [CrossRef]
9. Khomyakov, A.P.; Malinovskii, Y.A.; Sandomirskaya, S.M. Ferrotychite, $Na_6Fe_2(SO_4)(CO_3)_4$, a new mineral. *Zap. Vses. Mineral. Obshch.* **1981**, *110*, 600–603. (In Russian)
10. Khomyakov, A.P.; Bakhchisaraitsev, A.Y.; Martynova, A.V.; Parashchenko, T.M. Manganotychite $Na_6Mn_2(SO_4)(CO_3)_4$—A new mineral. *Zap. Vses. Mineral. Obshch.* **1990**, *119*, 46–49. (In Russian)
11. Sharygin, I.S.; Golovin, A.V.; Korsakov, A.V.; Pokhilenko, N.P. Tychite in Mantle Xenoliths from Kimberlites: The First Find and a New Genetic Type. *Dokl. Earth Sci.* **2016**, *467*, 270–274. [CrossRef]
12. Potapov, S.V.; Sharygin, I.S.; Konstantinov, K.M.; Danilov, B.S.; Shcherbakov, Y.D.; Letnikov, F.A. Melt Inclusions in Chromium Spinel of Kimberlites of the Zapolyarnaya Pipe, Upper Muna Field, Siberian Craton. *Dokl. Earth Sci.* **2022**, *504*, 271–275. [CrossRef]
13. Gossner, B.; Koch, I. Über das Kristallgitter von Langbeinit, Northupit und Hanksit. *Z. Kristallogr. Miner. Petrogr.* **1931**, *80*, 455–464.
14. Shiba, H.; Watanabé, T. Les structures des cristaux de northupite, de northupite bromée et de tychite. *Comptes Rend Hebd Acad. Sci.* **1931**, *193*, 1421–1423.
15. Watanabé, T. Les structures cristallines de la northupite $2MgCO_3{\cdot}2Na_2CO_3{\cdot}2NaCl$ et de la tychite $2MgCO_3{\cdot}2Na_2CO_3{\cdot}Na_2SO_4$. *Sci. Papers Inst. Phys. Chem. Res.* **1933**, *21*, 40–62.
16. Dal Negro, A.; Giuseppetti, G.; Tadini, C. Refinement of the crystal structure of northupite: $Na_3Mg(CO_3)_2Cl$. *Tscherm. Miner. Petrogr. Mitt.* **1975**, *22*, 158–163. [CrossRef]
17. Schmidt, G.R.; Jacqueline, R.; Yang, H.; Downs, R.T. Tychite, $Na_6Mg_2(SO_4)(CO_3)_4$: Structure Analysis and Raman Spectroscopic Data. *Acta Crystallogr.* **2006**, *E62*, i207–i209. [CrossRef]
18. Malinovskii, Y.A.; Baturin, S.V.; Belov, N.V. The crystal structure of the Fe-tychite. *Dokl. Akad. Nauk SSSR* **1979**, *249*, 1365–1368.
19. Palaich, S.E.M.; Manning, C.E.; Schauble, E.; Kavner, A. Spectroscopic and X-ray Diffraction Investigation of the Behavior of Hanksite and Tychite at High Pressures, and a Model for the Compressibility of Sulfate Minerals. *Am. Miner.* **2013**, *98*, 1543–1549. [CrossRef]
20. Sidorov, M.; Kompanchenko, A.; Fomina, E.; Kozlov, E. Raman Spectroscopic Study of Northupite Group Minerals (Tychite, Manganotychite, and Ferrotychite). *Zap. Ross. Mineral. Obshch.* **2022**, *151*, 94–101. (In Russian)
21. Zheng, Y.; Ellern, A.; Kögerler, P. A Spin-Frustrated Cobalt(II) Carbonate Pyrochlore Network. *Acta Crystallogr.* **2011**, *C67*, i56–i58. [CrossRef] [PubMed]
22. Fu, Z.; Zheng, Y.; Xiao, Y.; Bedanta, S.; Senyshyn, A.; Simeoni, G.G.; Su, Y.; Rücker, U.; Kögerler, P.; Brückel, T. Coexistence of Magnetic Order and Spin-Glass-like Phase in the Pyrochlore Antiferromagnet $Na_3Co(CO_3)_2Cl$. *Phys. Rev. B* **2013**, *87*, 214406. [CrossRef]
23. Nawa, K.; Okuyama, D.; Avdeev, M.; Nojiri, H.; Yoshida, M.; Ueta, D.; Yoshizawa, H.; Sato, T.J. Degenerate Ground State in the Classical Pyrochlore Antiferromagnet $Na_3Mn(CO_3)_2Cl$. *Phys. Rev. B* **2018**, *98*, 144426. [CrossRef]
24. Khomyakov, A.P. Mineralogical features of alkaline pegmatites of the Khibino-Lovozero Province. In *Development of Mineralogy and Geochemistry and Their Relation to the Science of Minerals*; Nauka: Moscow, Russia, 1983; pp. 66–82. (In Russian)
25. Panikorovskii, T.L.; Mikhailova, J.A.; Pakhomovsky, Y.A.; Bazai, A.V.; Aksenov, S.M.; Kalashnikov, A.O.; Krivovichev, S.V. Zr-Rich Eudialyte from the Lovozero Peralkaline Massif, Kola Peninsula, Russia. *Minerals* **2021**, *11*, 982. [CrossRef]
26. Agilent Technologies. *CrysAlisPro*; Version 1.171.36.20; Tokyo, Japan, 2012.
27. Sheldrick, G.M. A short history of SHELX. *Acta Crystallogr.* **2008**, *A64*, 112–116. [CrossRef] [PubMed]
28. Hawthorne, F.C.; Krivovichev, S.V.; Burns, P.C. The Crystal Chemistry of Sulfate Minerals. *Rev. Miner. Geochem.* **2000**, *40*, 1–112. [CrossRef]
29. Alexandrov, E.V.; Blatov, V.A.; Kochetkov, A.V.; Proserpio, D.M. Underlying Nets in Three-Periodic Coordination Polymers: Topology, Taxonomy and Prediction from a Computer-Aided Analysis of the Cambridge Structural Database. *CrystEngComm* **2011**, *13*, 3947–3958. [CrossRef]
30. Krivovichev, S.V.; Filatov, S.K. Structural Principles for Minerals and Inorganic Compounds Containing Anion-Centered Tetrahedra. *Am. Mineral.* **1999**, *84*, 1099–1106. [CrossRef]
31. Krivovichev, S.V. Minerals with antiperovskite structure: A review. *Z. Kristallogr.* **2008**, *223*, 109–113. [CrossRef]
32. Bailey, M.S.; Shen, D.Y.; McGuire, M.A.; Fredrickson, D.C.; Toby, B.H.; DiSalvo, F.J.; Yamane, H.; Sasaki, S.; Shimada, M. The Indium Subnitrides $Ae_6In_4(In_xLi_y)N_{3-z}$ (*Ae* = Sr and Ba). *Inorg. Chem.* **2005**, *44*, 6680–6690. [CrossRef]
33. Pathak, M.; Stoiber, D.; Bobnar, M.; Ovchinnikov, A.; Ormeci, A.; Niewa, R.; Höhn, P. Synthesis, Characterization, and Chemical Bonding Analysis of the Lithium Alkaline-Earth Metal Gallide Nitrides $Li_2(Ca_3N)_2[Ga_4]$ and $Li_2(Sr_3N)_2[Ga_4]$. *Z. Anorg. Allg. Chem.* **2017**, *643*, 1557–1563. [CrossRef]
34. Leonard, S.R.; Snyder, B.S.; Brewer, L.; Stacy, A.M. Structure Determinations of Two New Ternary Oxides: Ti_3PdO and Ti_4Pd_2O. *J. Solid State Chem.* **1991**, *92*, 39–50. [CrossRef]
35. Krivovichev, S.V. Topological complexity of crystal structures: Quantitative approach. *Acta Crystallogr.* **2012**, *A68*, 393–398. [CrossRef]

36. Krivovichev, S.V. Structural complexity of minerals: Information storage and processing in the mineral world. *Miner. Mag.* **2013**, *77*, 275–326. [CrossRef]
37. Krivovichev, S.V.; Krivovichev, V.G.; Hazen, R.M.; Aksenov, S.M.; Avdontceva, M.S.; Banaru, A.M.; Gorelova, L.A.; Ismagilova, R.M.; Kornyakov, I.V.; Kuporev, I.V.; et al. Structural and chemical complexity of minerals: An update. *Mineral. Mag.* **2022**, *86*, 183–204. [CrossRef]
38. Kampf, A.R.; Rossman, G.R.; Ma, C.; Belmonte, D.; Biagioni, C.; Castellaro, F.; Chiappino, L. Ramazzoite, $[Mg_8Cu_{12}(PO_4)(CO_3)_4(OH)_{24}(H_2O)_{20}][(H_{0.33}SO_4)_3(H_2O)_{36}]$, the first mineral with a polyoxometalate cation. *Eur. J. Mineral.* **2018**, *30*, 827–834. [CrossRef]
39. Elliott, P.; Giester, G.; Rowe, R.; Pring, A. Putnisite, $SrCa_4Cr^{3+}{}_8(CO_3)_8SO_4(OH)_{16}\cdot 25H_2O$, a new mineral from Western Australia: Description and crystal structure. *Mineral. Mag.* **2014**, *78*, 131–144. [CrossRef]
40. Krivovichev, S.V. Polyoxometalate clusters in minerals: Review and complexity analysis. *Acta Crystallogr.* **2020**, *B76*, 618–629. [CrossRef]
41. Hazen, R.M.; Morrison, S.M. On the paragenetic modes of minerals: A mineral evolution perspective. *Am. Miner.* **2022**, *107*, 1262–1287. [CrossRef]